



IVANNIKOV ISP RAS OPEN CONFERENCE

**ISP RAS – 25 years in IT
MOSCOW, 5-6 DECEMBER, 2019**

Numerical experiments with the coupled ocean-earth-atmosphere circulation model and the analysis of decadal variability of its main physical characteristic

Natalia Tuchkova¹, Konstantin Belyaev^{1,2}, Gury Mikhailov¹

¹*Dep. of Computational Systems and Scientific Information Federal Research Center CSC, RAS, Moscow, Russia*

²*Laboratory of hydrological processes Shirshov Institute of Oceanology, RAS Moscow, Russia*

Supported in part by FASO Russia themes: RFBR 18-29-10085МК; #0128-2019-0011 (IO RAS) and "Mathematical methods of data analysis and forecasting" (FRC CSC RAS)

Outline of work

The work carried out **ensemble computational experiments** with the model MPI-ESM of the Institute of Meteorology named after M. Planck (German Climate Computing Center, Hamburg, Germany).

A series of **different initial values** of characteristic fields (drifting stations GFDL, PIRATA, etc.) were set and the model integrated, starting with each of these fields for 10 and more years.

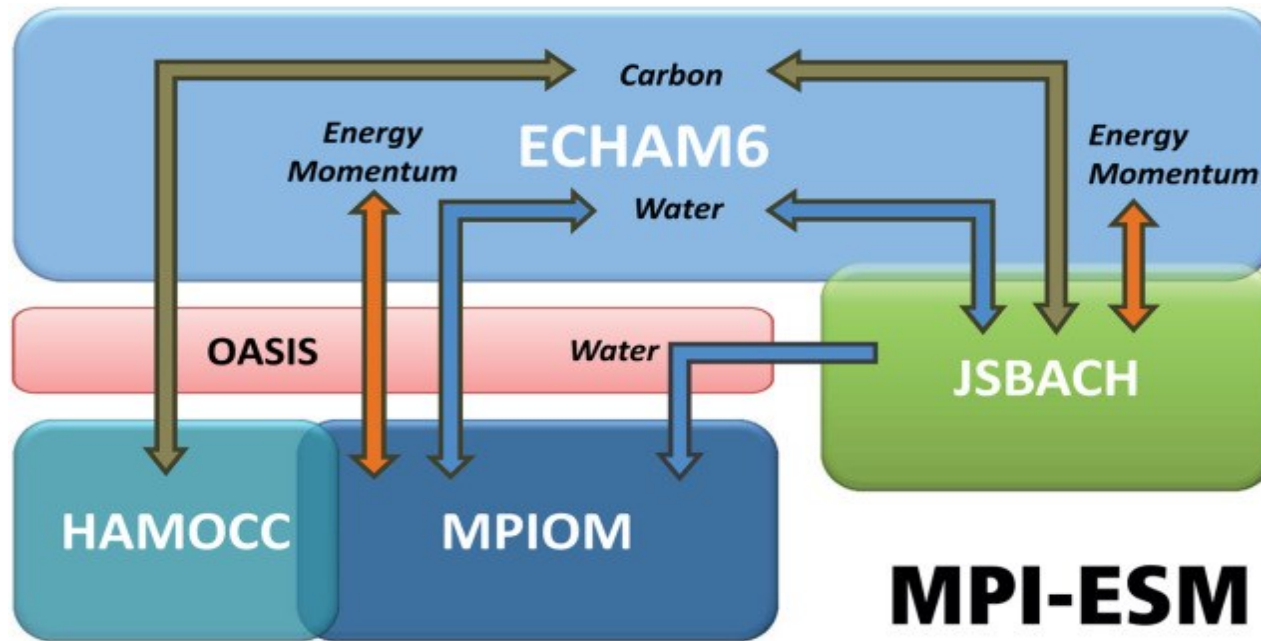
The behavior of the **average field from** these calculations, the characteristics of deviations of model calculations from the average field, the most probable paths of a number of characteristics, the behavior of distributions of some parameters and a number of other tasks were studied.

The **stability of model calculations** to perturbation of initial fields was also assessed.

Numerical calculations were performed on the supercomputers Mistral (DKRZ, Hamburg, Germany) and Lomonosov-2 (Lomonosov Moscow State University, Moscow, Russia).

Model characteristics of the Russian Arctic zone were analyzed.

Schematic view of MPI-ESM



Colored boxes show the model components:

ECHAM6 is the **atmospheric** general circulation model, which is directly coupled to the JSBACH and model that describes **physical and biogeochemical** aspects of soil and vegetation. MPIOM is the **ocean general circulation model**, which includes the HAMOCC model for the **marine biogeochemistry**.

OASIS is the **coupler program**, which aggregates, interpolates, and exchanges fluxes and state variables once a day between ECHAM6+JSBACH and MPIOM+HAMOCC.

The coupler exchanges fluxes for water, energy, momentum, and CO₂.

MPI-ESM Configuration	ECHAM6 Resolution	MPIOM Resolution	JSBACH Vegetation	Orbit
LR	T63/1.9° L47	GR15 L40	Dynamic	VSOP87
MR	T63/1.9° L95	TP04 L40	Dynamic	VSOP87
P	T63/1.9° L47	GR15 L40	Prescribed	Kepler

- Depending on the experiment, the model was set to use different spatial resolutions.
- **T63L47/GR15L40 (“LR” - Low Resolution)**
 - Atmosphere: approximate **horizontal resolution of 200 km** (1.875 degrees) at **47 layers** (up to 0.01 hPa / 80 km in height)
 - Land biosphere (interactive vegetation): same horizontal resolution as atmosphere
 - Ocean including biogeochemistry: horizontal resolution varies from 12 to 150 km at 40 layers
- **T63L95/TP04L40 (“MR” - Mixed Resolution)**
 - Atmosphere: approximate **horizontal resolution of 200 km** (1.875 degrees) and **higher vertical resolution of 95 layers** (up to 0.01 hPa / 80 km in height)
 - Land biosphere (interactive vegetation): same horizontal resolution as atmosphere
 - Ocean including biogeochemistry: horizontal resolution varies from an average of 0.4 degrees (40 km) at 40 layers

MPI-ESM-HR

Name	Atmosphere resolution	Ocean resolution	Ocean mixing scheme	Description
HR	T127 (0.93° or ~ 103 km)	TP04 (0.4° or ~ 44 km)	PP, KPP	Reference, ocean mixing sensitivity
XR	T255 (0.46° or ~ 51 km)	TP04 (0.4° or ~ 44 km)	PP, KPP	Increased atmospheric resolution, ocean mixing sensitivity
ER	T127 (0.93° or ~ 103 km)	TP6M (0.1° or ~ 11 km)	PP	Increased ocean resolution

The number of **vertical levels is 95 in the atmosphere and 40 in the ocean**, respectively. In brackets, the nominal horizontal resolution in a Gaussian grid (approximated at the Equator) is given.

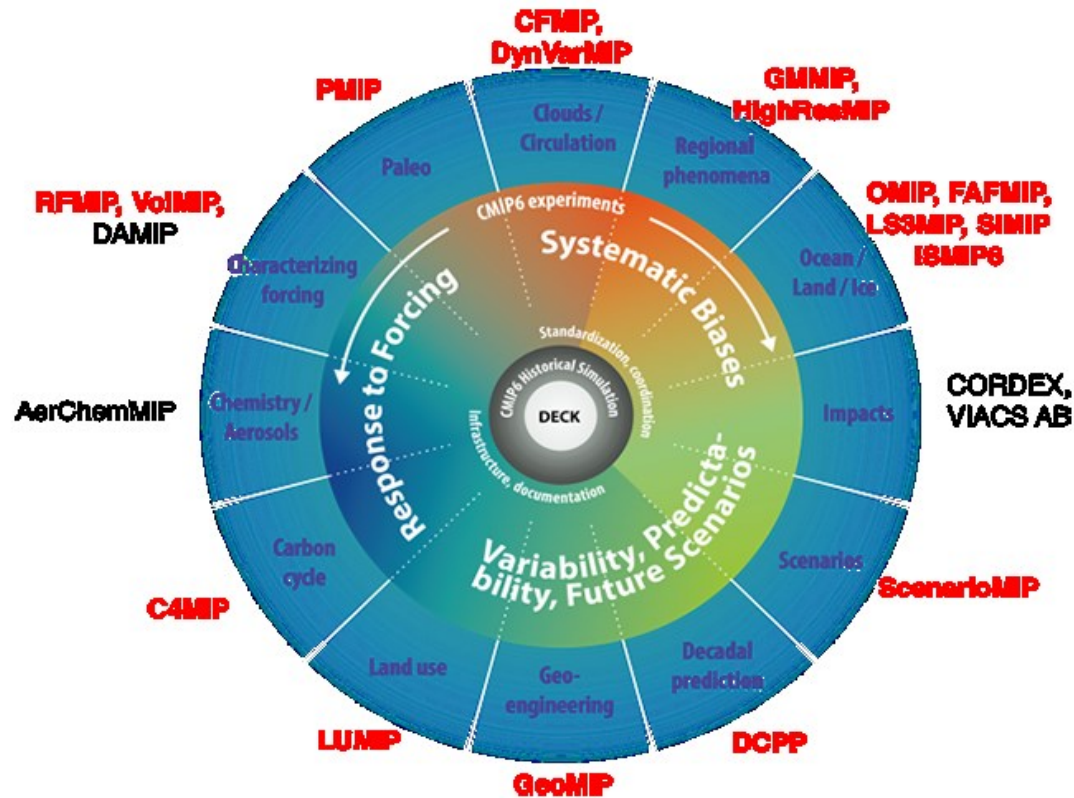
The simulations follow the High Resolution Model Intercomparison Project (HighResMIP) protocol and provide climate simulations with varying horizontal resolutions that are higher than the standard resolution of the **Coupled Model Intercomparison Project – phase 6 (CMIP6)**. The reference model is the MPI-ESM1.2-HR, which was described by [Müller e](#)

Müller, W. A., Jungclaus, J. H., Mauritsen, T., Baehr, J., Bittner, M., Budich, R., Bunzel, F., Esch, M., Ghosh, R., Haak, H., Ilyina, T., Kleine, T., Kornblueh, L., Li, H., Modali, K., Notz, D., Pohlmann, H., Roeckner, E., Stemmler, I., Tian, F., and Marotzke, J.: A higher-resolution version of the Max Planck Institute Earth System Model (MPI-ESM 1.2-HR), *J. Adv. Model. Earth Sy.*, 10, 1383–1413, <https://doi.org/10.1029/2017MS001217>, 2018. [a](#), [b](#), [c](#), [d](#), [e](#), [f](#), [g](#), [h](#), [i](#), [j](#)

The spin-up with the coupled model of MPI-ESM-HR is performed with preindustrial conditions (from 1850 to 1990) and next period were with data assimilation (up to 2027)

Coupled Model Intercomparison Project – phase 6 (CMIP6)

<https://www.climateurope.eu/cmip6-wcrp-coupled-model-intercomparison-project-phase-6/>

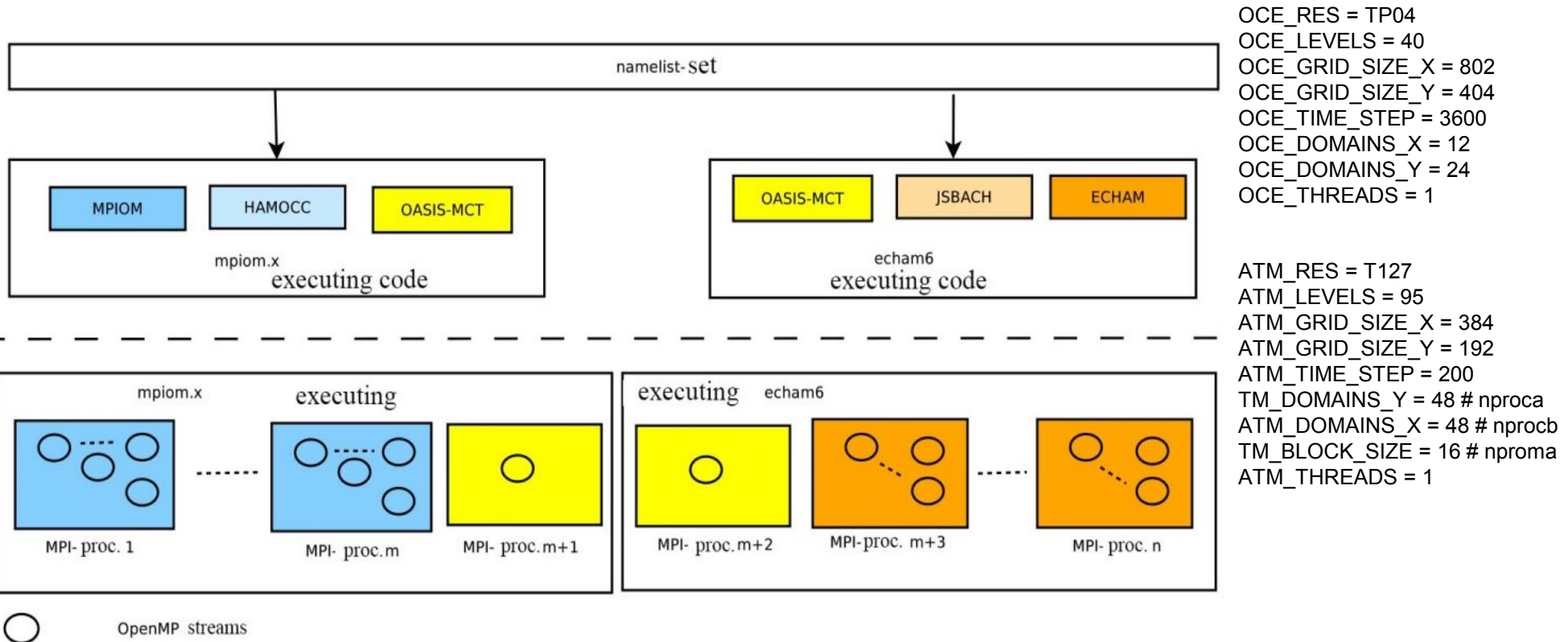


Schematic of the CMIP6 experiment design (Eyring et al., 2016). The inner ring and surrounding white text involve standardized functions of all CMIP DECK experiments and the CMIP6 historical simulation. The middle ring shows science topics related specifically to CMIP6, which are addressed by the CMIP6-endorsed MIPs. The topics and MIPs are shown in the outer ring, where MIPs with active participation by the MPI-M are highlighted in red.

Eyring, V., Bony, S., Meehl, G. A., Senior, C. A., Stevens, B., Stouffer, R. J., and Taylor, K. E.: Overview of the Coupled Model Intercomparison Project Phase 6 (CMIP6) experimental design and organization, *Geosci. Model Dev.*, 9, 1937–1958, <https://doi.org/10.5194/gmd-9-1937-2016>, 2016.

Diagram of multiprocessor organization of numerical experiments with MPI-ESM-HR Mistral DKRZ

MODEL_ID = MPI-ESM-HR, ntasks=2592, PARENT_EXP_ID = cmip6_spinup-HR



Code execution stages; an initiation step and a calculation step are shown; are passed preprocessing, preprocessing, visualization stages (*Salnikov A.N. et al. 2016*)

Salnikov A. N., Tchkova N. P., Kirchner I. European model of climate change: Architecture and features of deployment on Russian supercomputers // *CEUR Workshop Proceedings*. 2016. Vol. 1576. P. 678–684.

The basic equations defining the **ocean block** of MPI-ESM

This system is solved numerically in a 2D-grid for the selected z levels. The boundary conditions are set by the parameters of the atmosphere (sea surface) and are taken from a model of the atmosphere, which simulates wind strength, heat fluxes and precipitation (freshwater flows).

$$\begin{aligned}
 \frac{\partial u}{\partial t} + u \frac{\partial u}{\partial x} + v \frac{\partial u}{\partial y} + w \frac{\partial u}{\partial z} + fv &= -\frac{\partial P}{g\rho_0 \partial x} + \kappa \Delta u \\
 \frac{\partial v}{\partial t} + u \frac{\partial v}{\partial x} + v \frac{\partial v}{\partial y} + w \frac{\partial v}{\partial z} - fu &= -\frac{\partial P}{g\rho_0 \partial y} + \kappa \Delta v \\
 \frac{\partial u}{\partial x} + \frac{\partial v}{\partial y} + \frac{\partial w}{\partial z} &= 0 \\
 \frac{\partial \theta}{\partial t} + u \frac{\partial \theta}{\partial x} + v \frac{\partial \theta}{\partial y} + w \frac{\partial \theta}{\partial z} &= \mu \Delta \theta \\
 \frac{\partial S}{\partial t} + u \frac{\partial S}{\partial x} + v \frac{\partial S}{\partial y} + w \frac{\partial S}{\partial z} &= \mu \Delta S \\
 \rho &= \rho(\theta, S, P)
 \end{aligned} \tag{1}$$

System of equations (1) determines the state of the ocean at any time t at the point (x, y, z) of space (grid). Hereafter, the standard notations are used. Namely u, v, w are the components of the velocity vector, respectively, in the north, east and vertical (down) directions. Symbols θ, S, ρ indicate the potential temperature, salinity and density. P indicates pressure, ρ_0 is the corresponding average density value for the selected level z ; g is the acceleration of gravity; f is the Coriolis parameter, equal to $f = 2\Omega \sin \phi$, where Ω is the angular velocity of the Earth's rotation ($7.2921 \times 10^{-5} \text{s}^{-1}$) around the axis; ϕ is the geographical latitude of the place; μ, κ are the viscosity coefficients for speed and temperature (salinity) in equations (1); Δ is the standard Laplace 2D-operator.

Data assimilation scheme (Belyaev K.P. et al., 2018).

X_a – after, X_b – before,
 K – Kalman – gain, Q – covariation

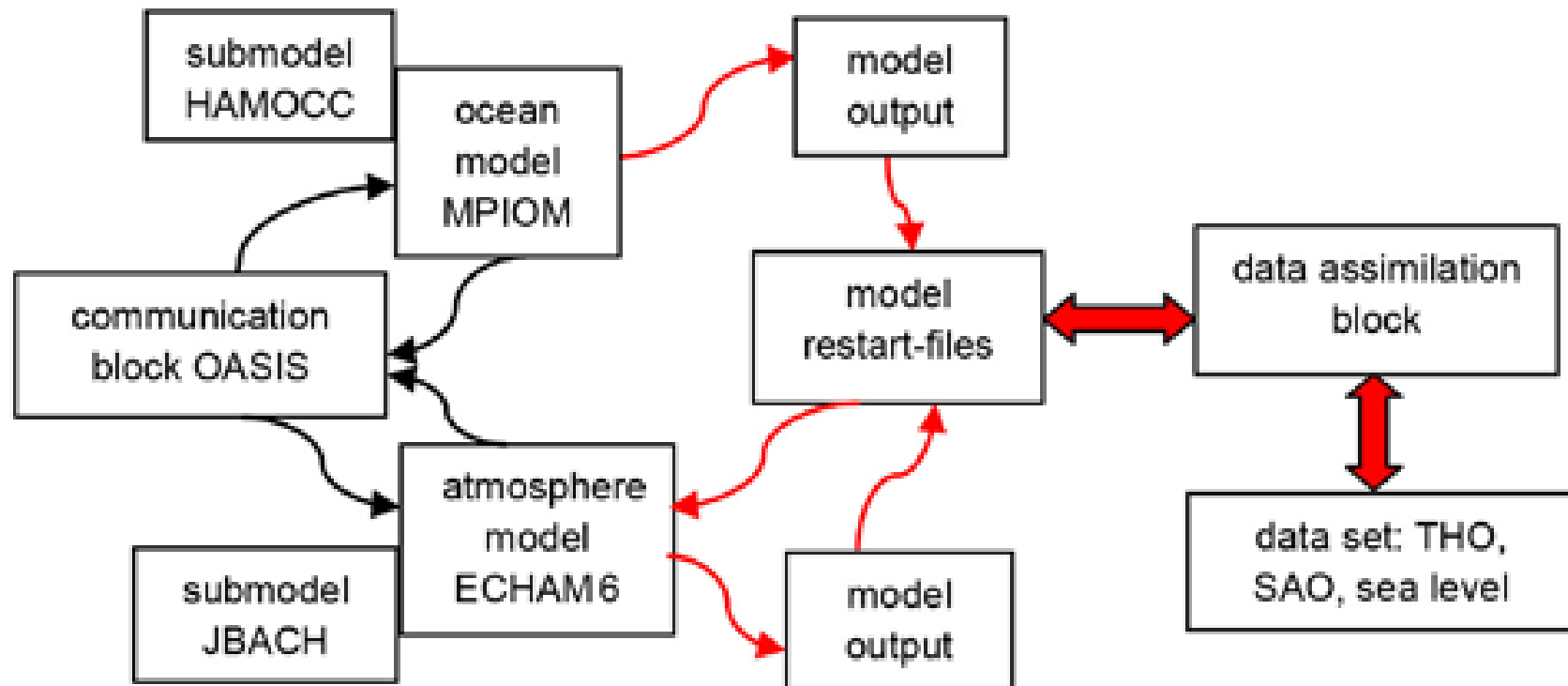
$$K = \sigma^{-1} (\Lambda - C)(H\Lambda)^T Q^{-1}$$

$$X_a = X_b + K (Y - HX_b)$$

$$\sigma = (H\Lambda)^T Q^{-1} (H\Lambda),$$

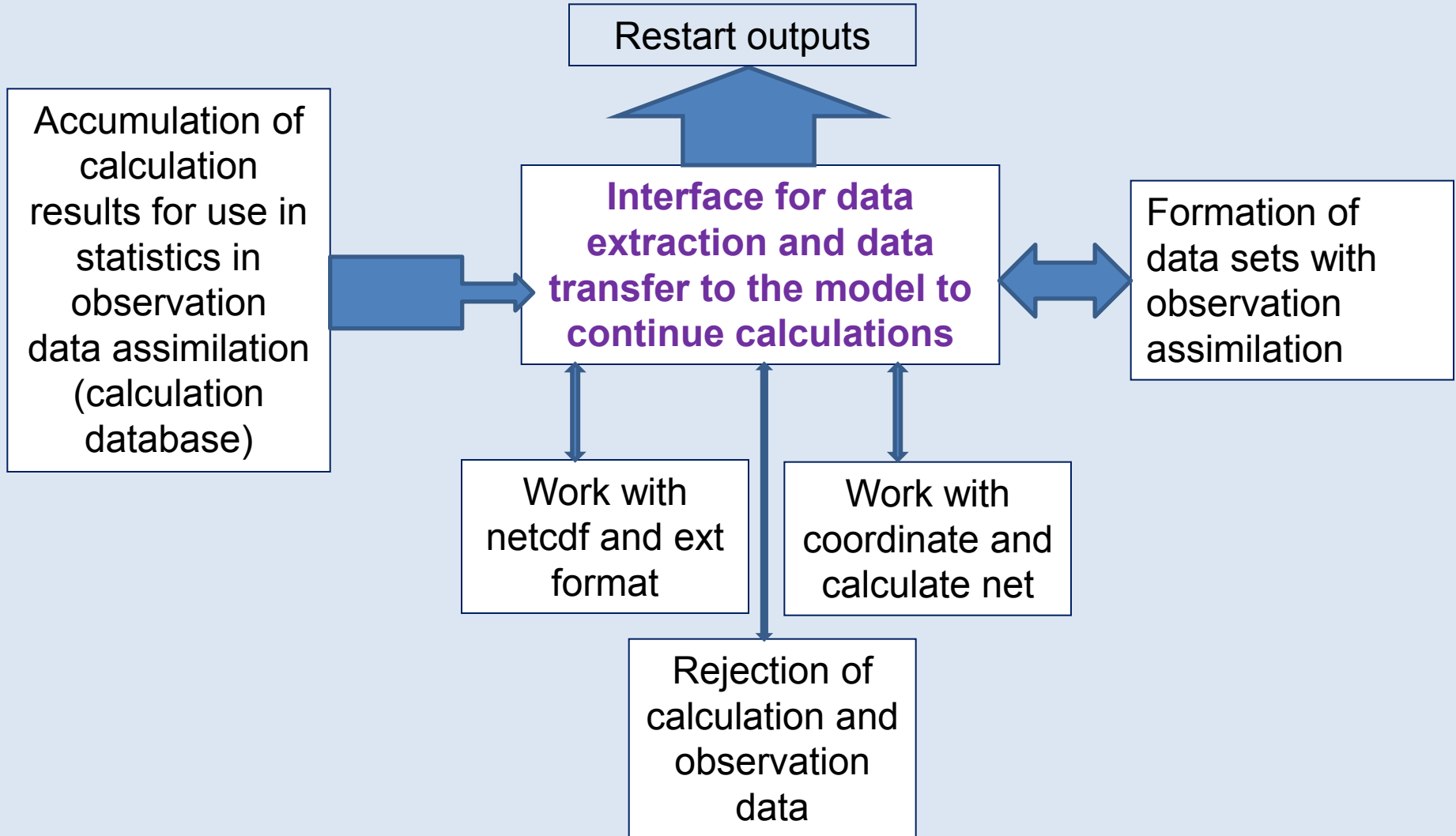
Belyaev K.P., Kirchner I., Kuleshov A.A., Tuchkova N.P. Numerical Realization of Hybrid Data Assimilation Algorithm in Ensemble Experiments with the MPIESM Coupled Model. In: Velarde M., Tarakanov R., Marchenko A. (eds). The Ocean in Motion. Springer Oceanography. 2018. P. 447-459. https://doi.org/10.1007/978-3-319-71934-4_27.

Data assimilation modules into MPI-ESM-HR (Belyaev K.P. et al., 2016)

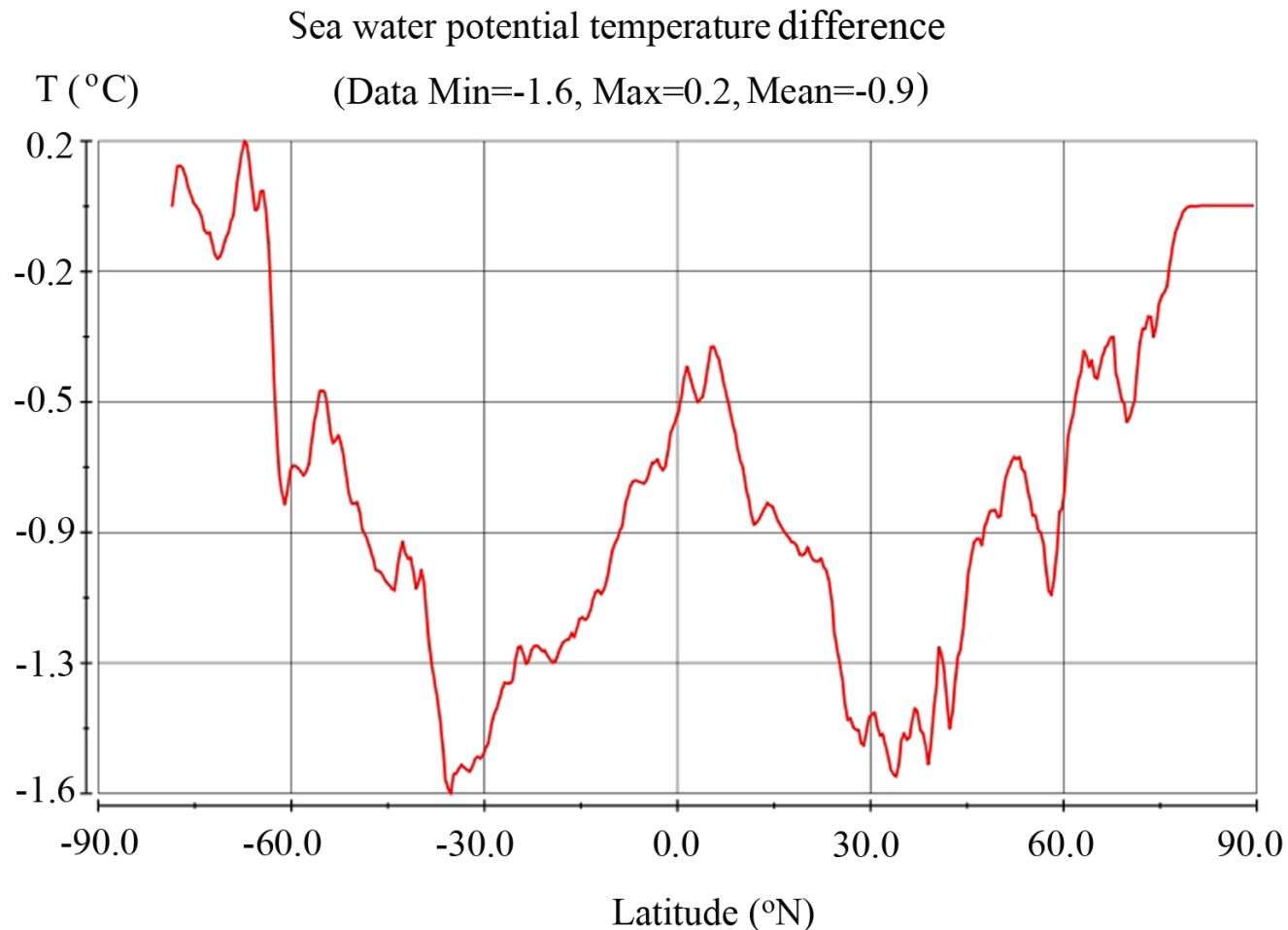


Belyaev K.P., Kuleshov A.A., Kirchner I., Tuchkova N.P. Data assimilation experiments with MPIESM climate model // MATEC Web of Conferences **76**, 05003 (2016) <https://doi.org/10.1051/matecconf/20167605003>

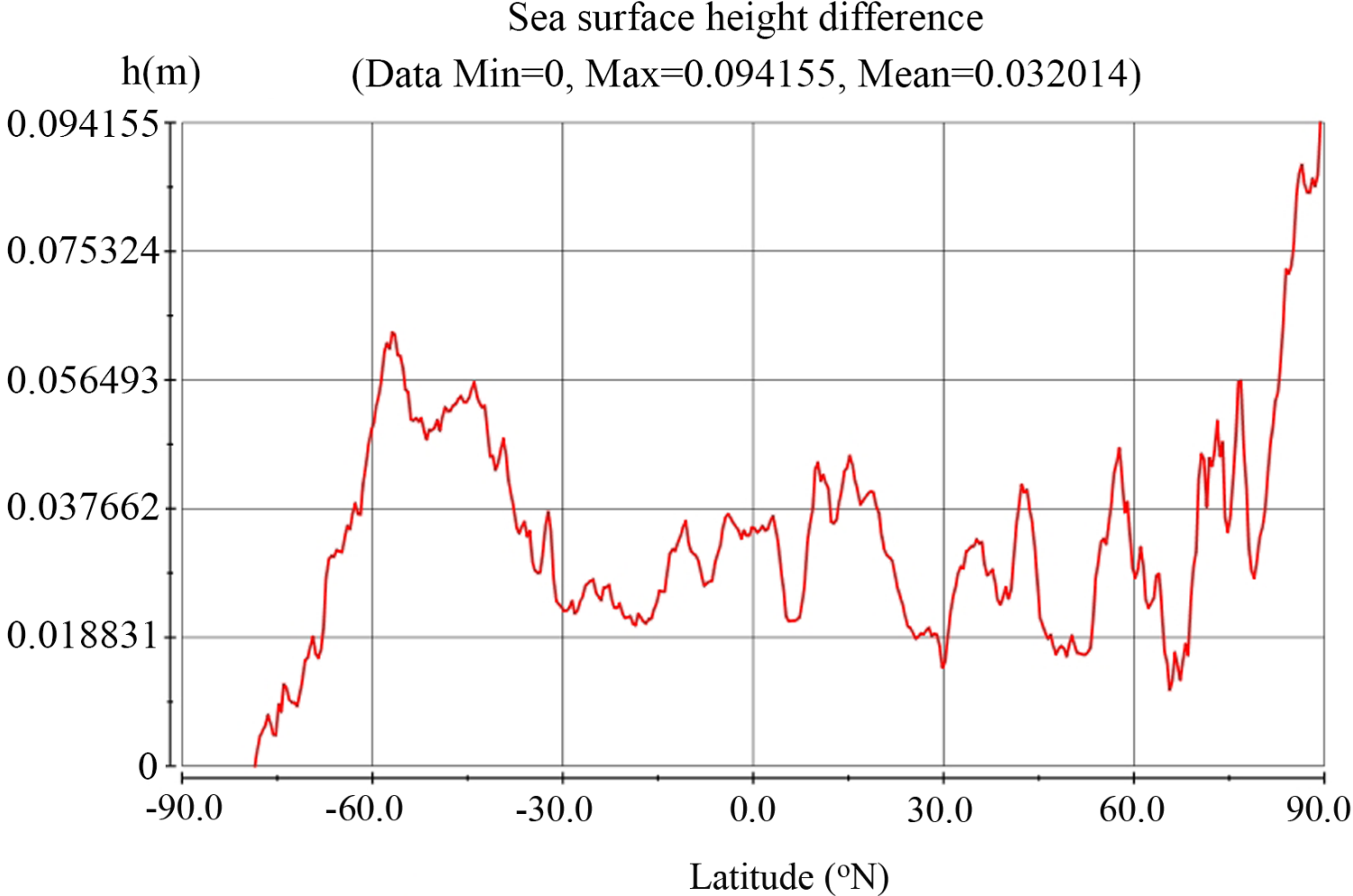
Data assimilation block



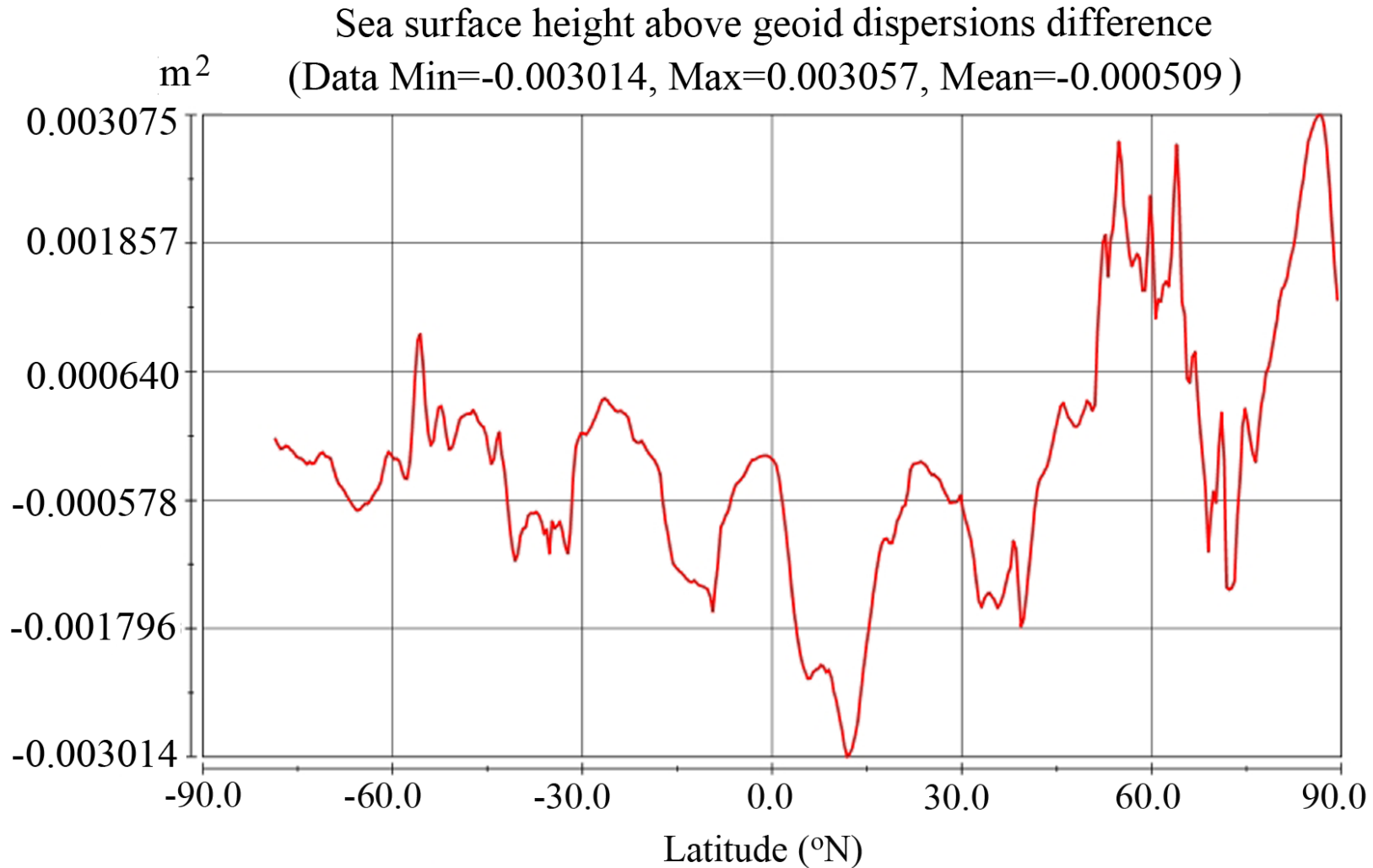
The difference in maximum temperature deviations from the average on the surface in January 1990-2000



The curve of the difference between the maximum deviations relative to the average ocean level before and after integration in January 1990-2000

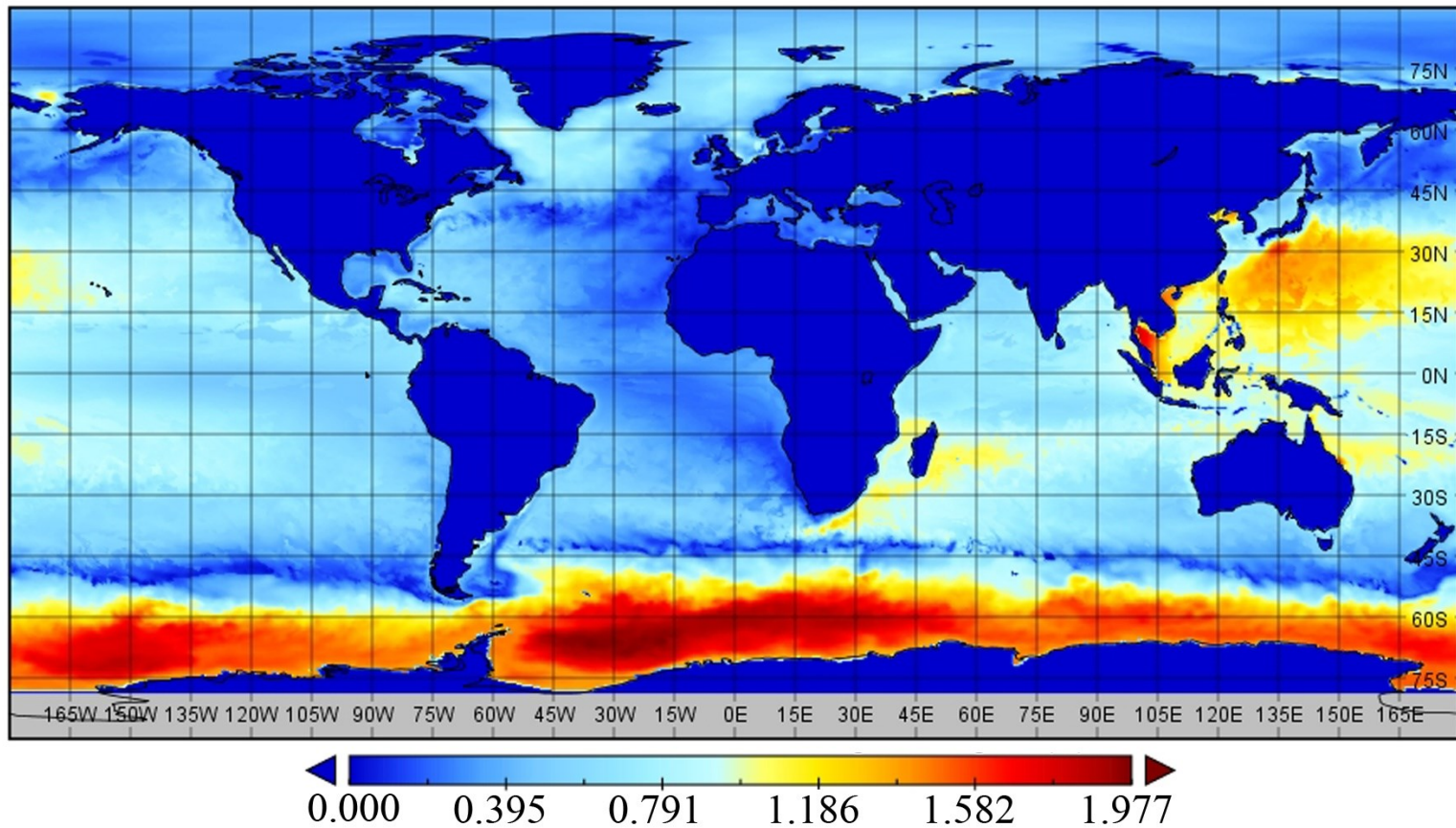


The deviation field of ocean level dispersions before and after integration in January 1990-2000



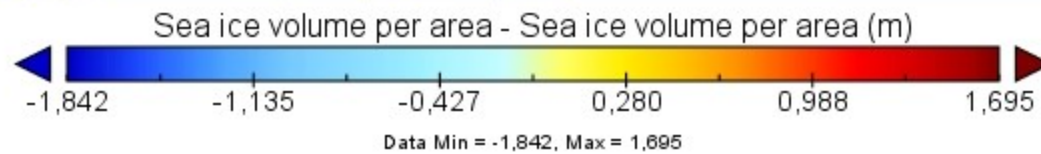
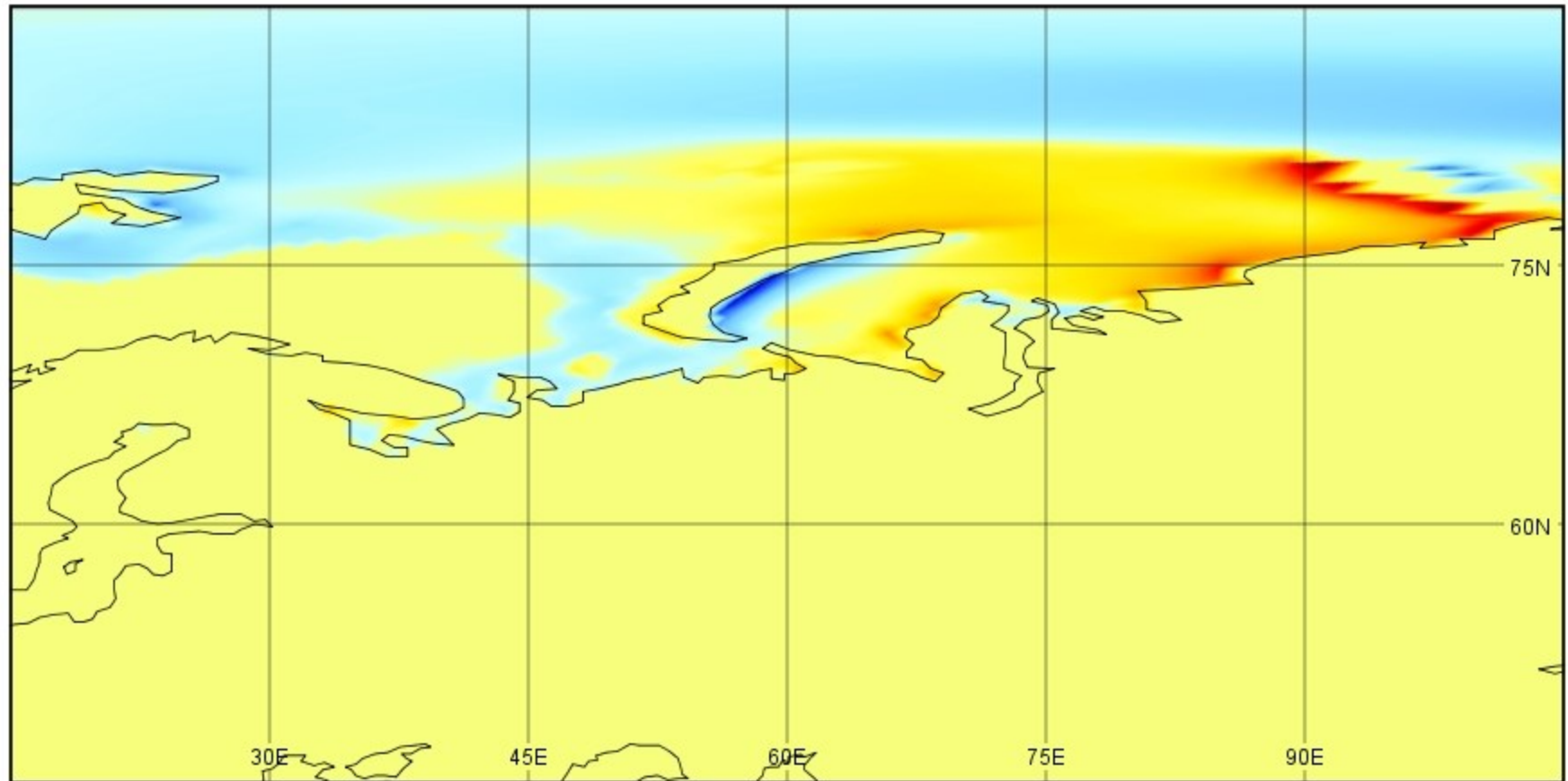
The field of difference of the minimum deviations relative to the average ocean level fields before and after integration in January 1990-2000

Sea surface height above geoid (m) (Data Min = 0, Max = 1.977, Mean = 0.504)



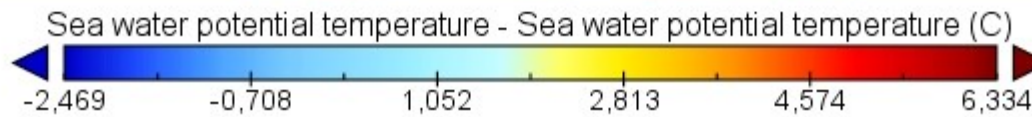
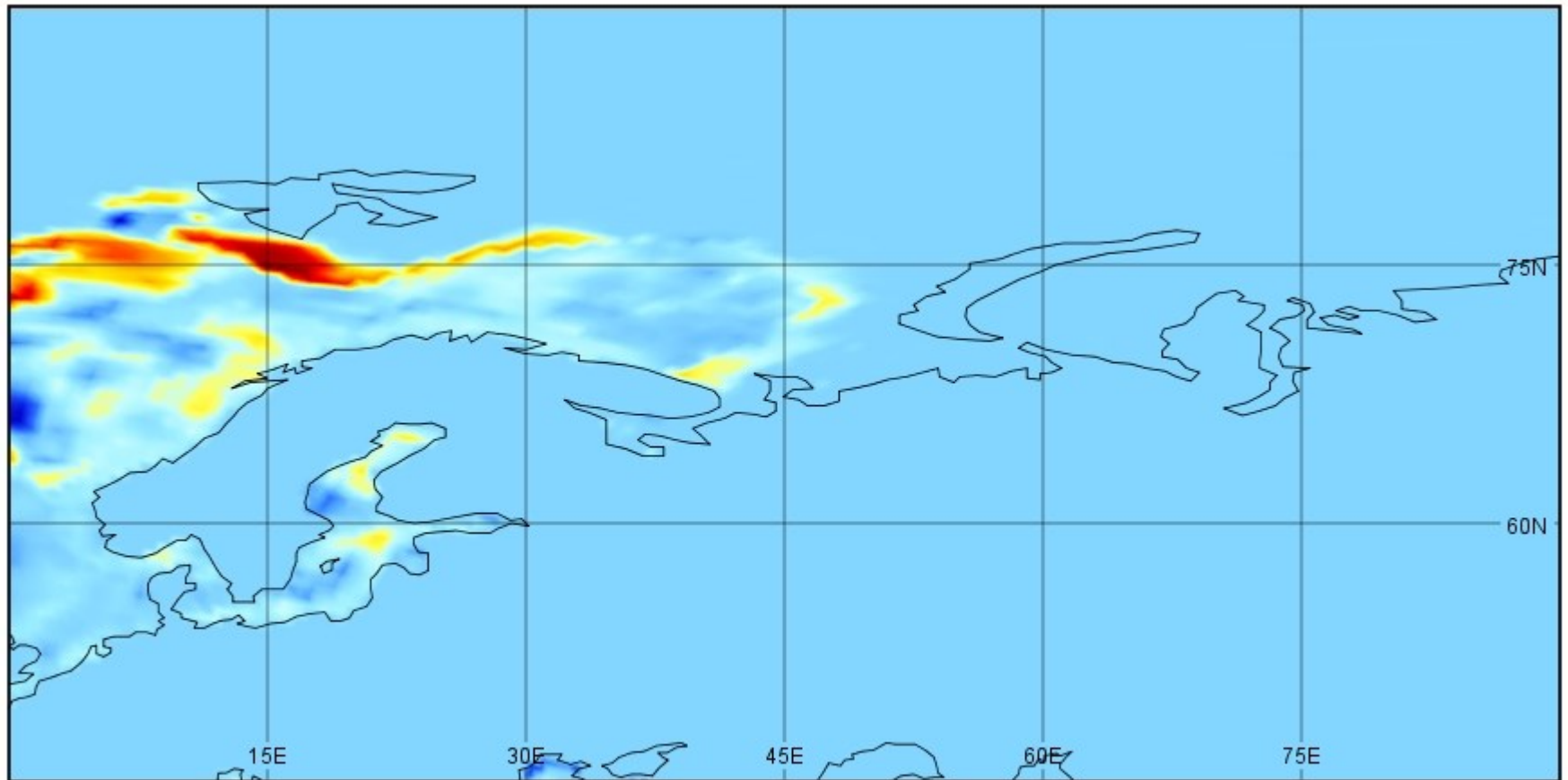
Difference in ice volume in the Russian Arctic 2011-2027 (MPI-ESM-HR forecast) in January

Sea ice volume per area

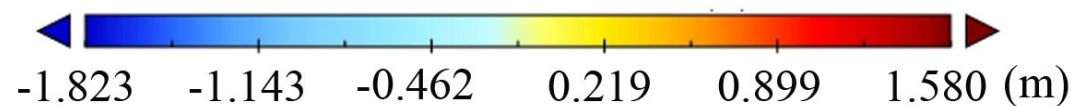
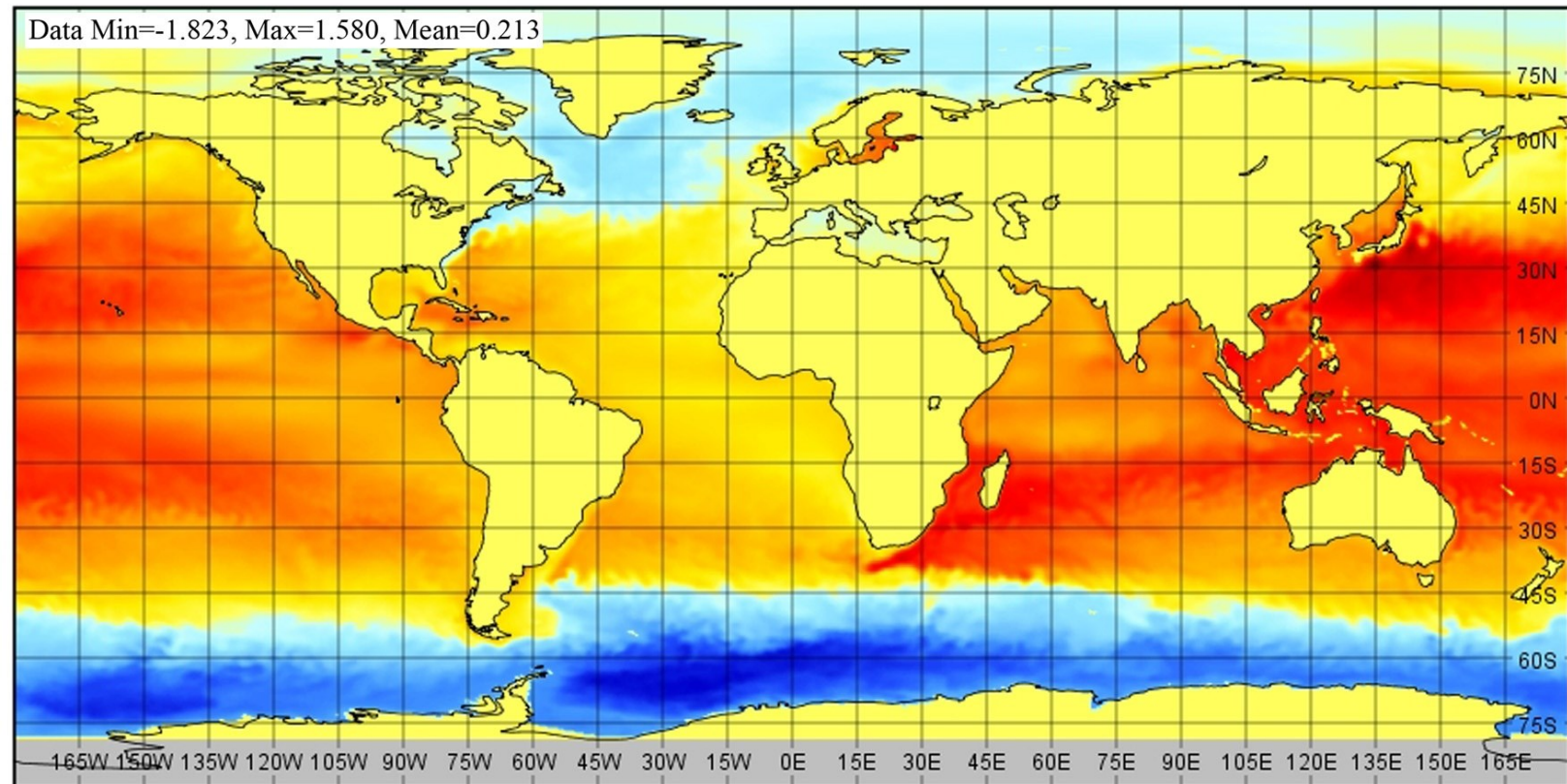


Difference in potential surface temperature in the Russian Arctic 2011-2027 (MPI-ESM-HR forecast) in January

Sea water potential temperature

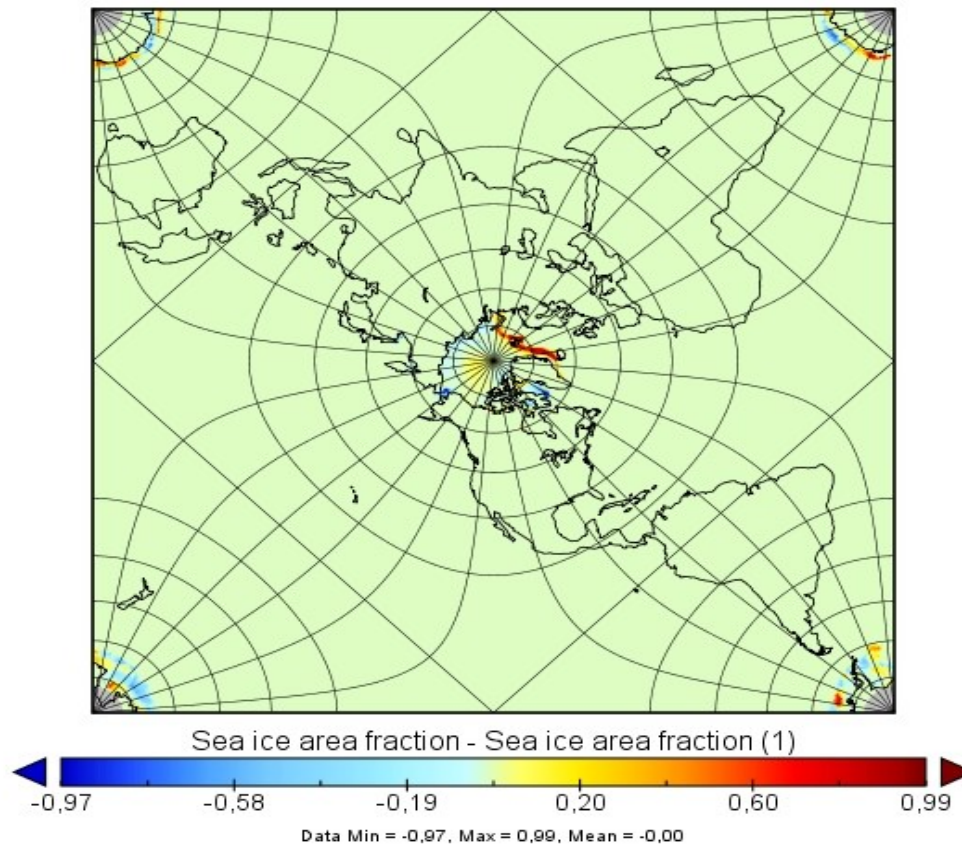


Model forecast of ocean level (meters) 2000-2027 years in January

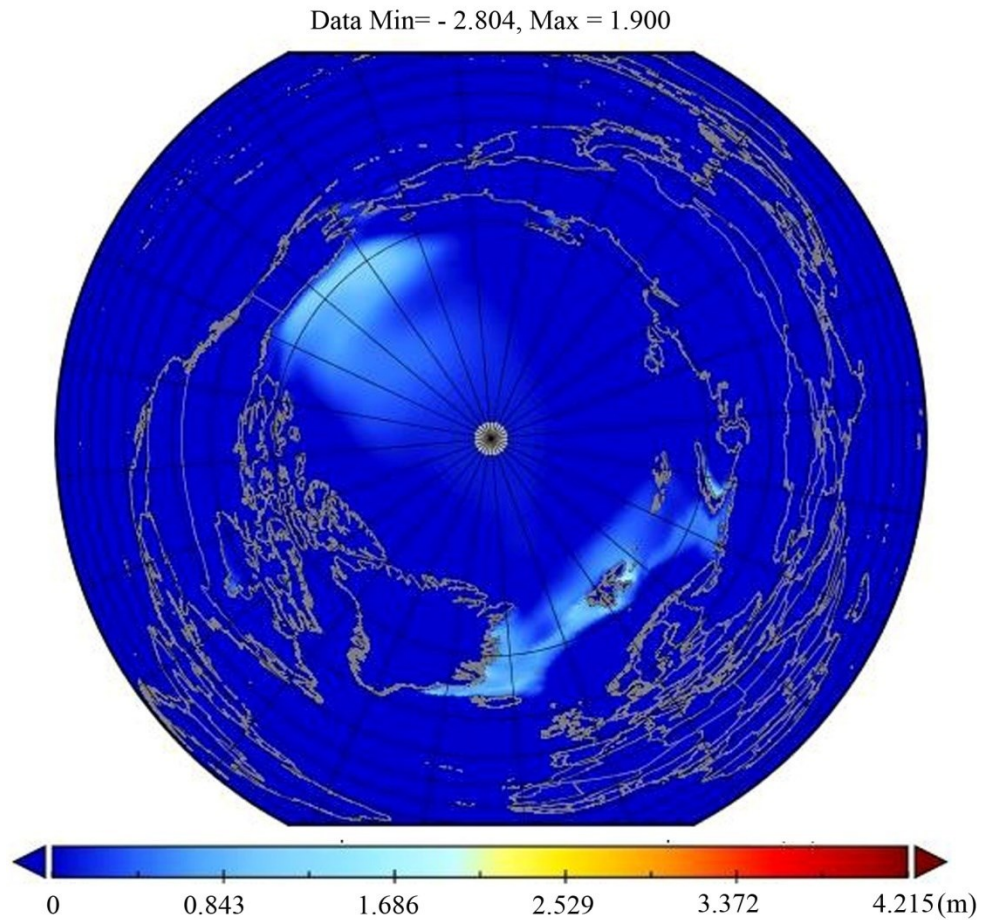


Arctic ice fraction - difference with model calculation after 11 months of run at assimilation of temperature and salinity data 6 experiments in November 1992-1993

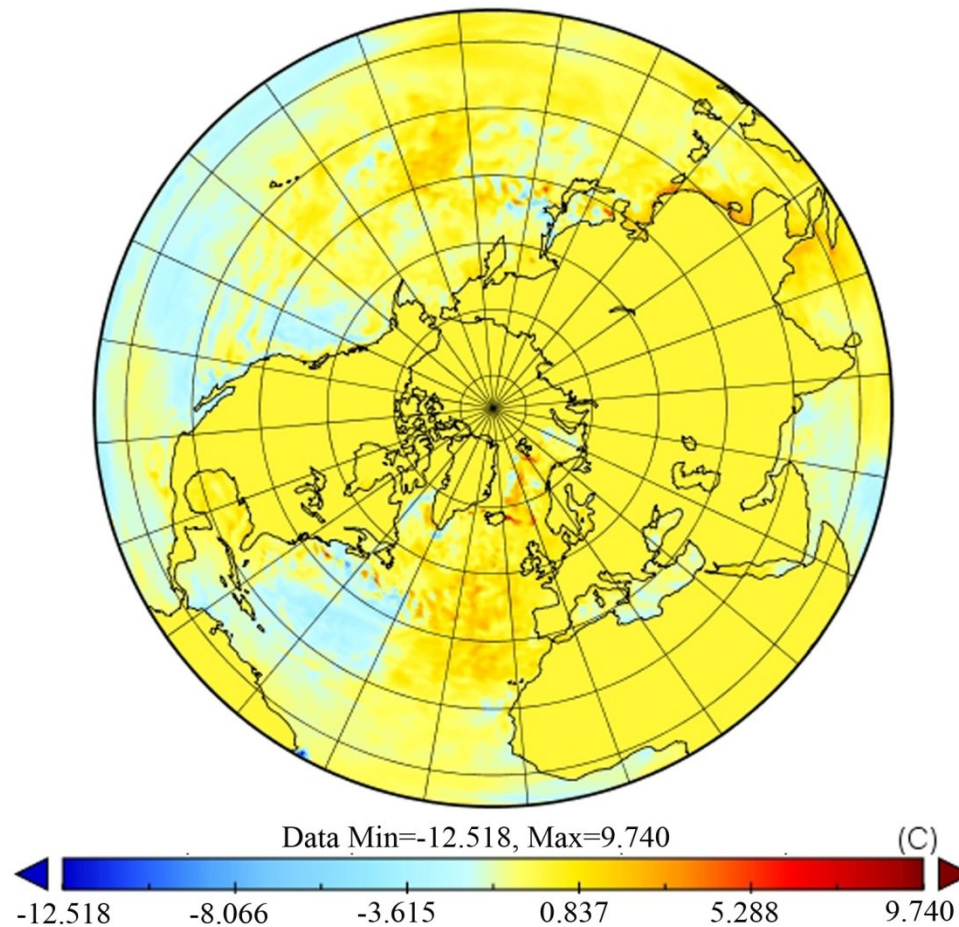
Sea ice area fraction (assimilation-model) after 11 months



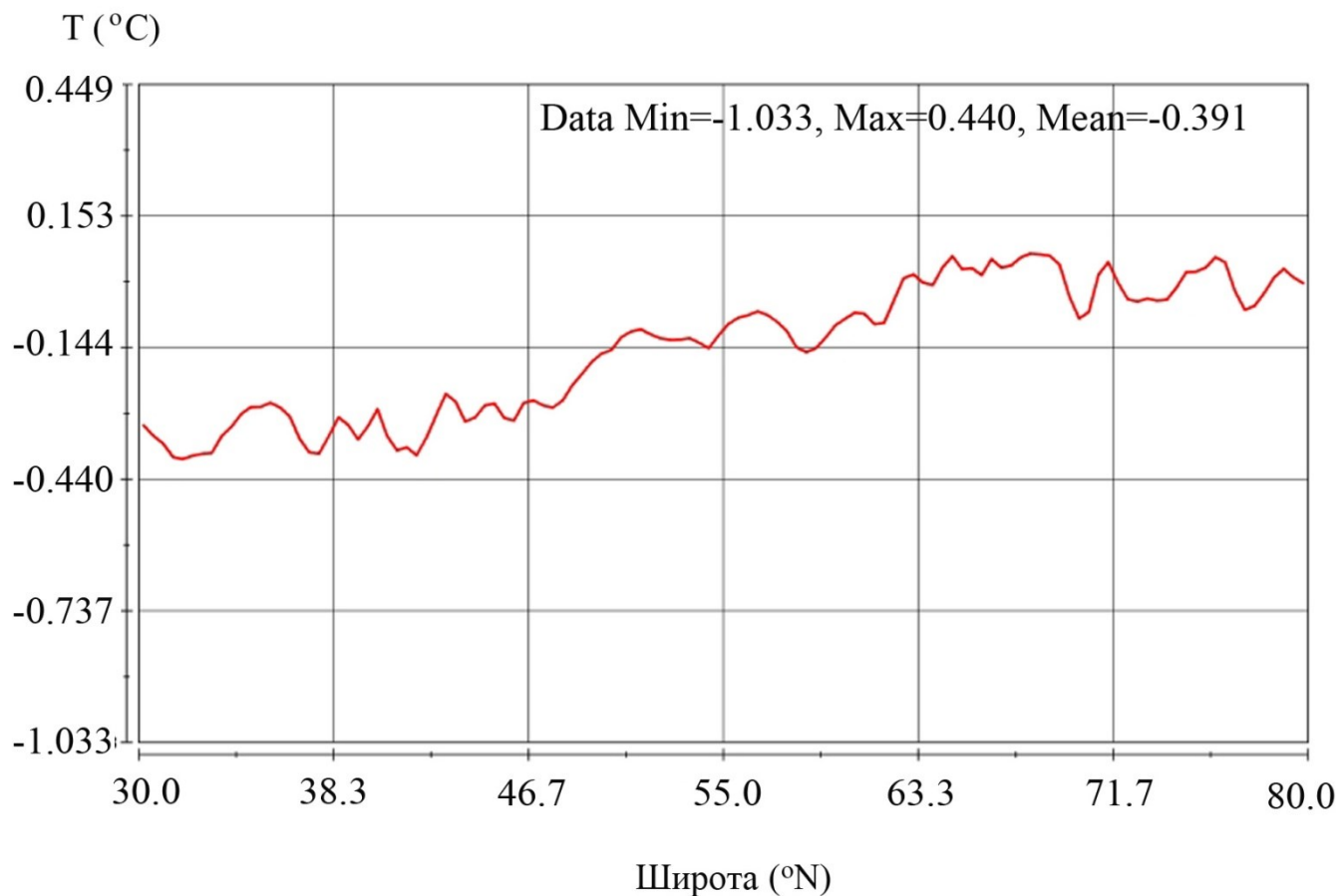
Model forecast (MPI-ESM-HR) of ice change on the Arctic sea surface 1990-2027 in January



Arctic potential surface temperature difference 2000-2027 (MPI-ESM-HR forecast) in January

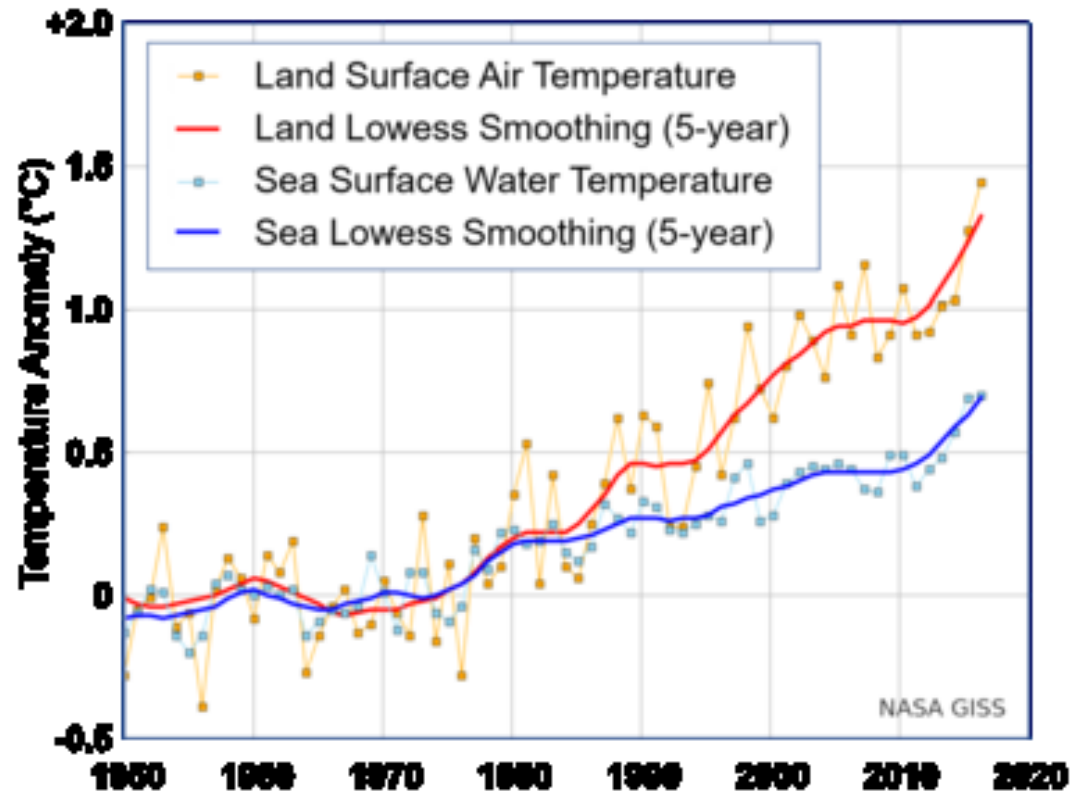


Arctic potential temperature rise curve 2000-2027 (model forecast MPI-ESM-HR) in January



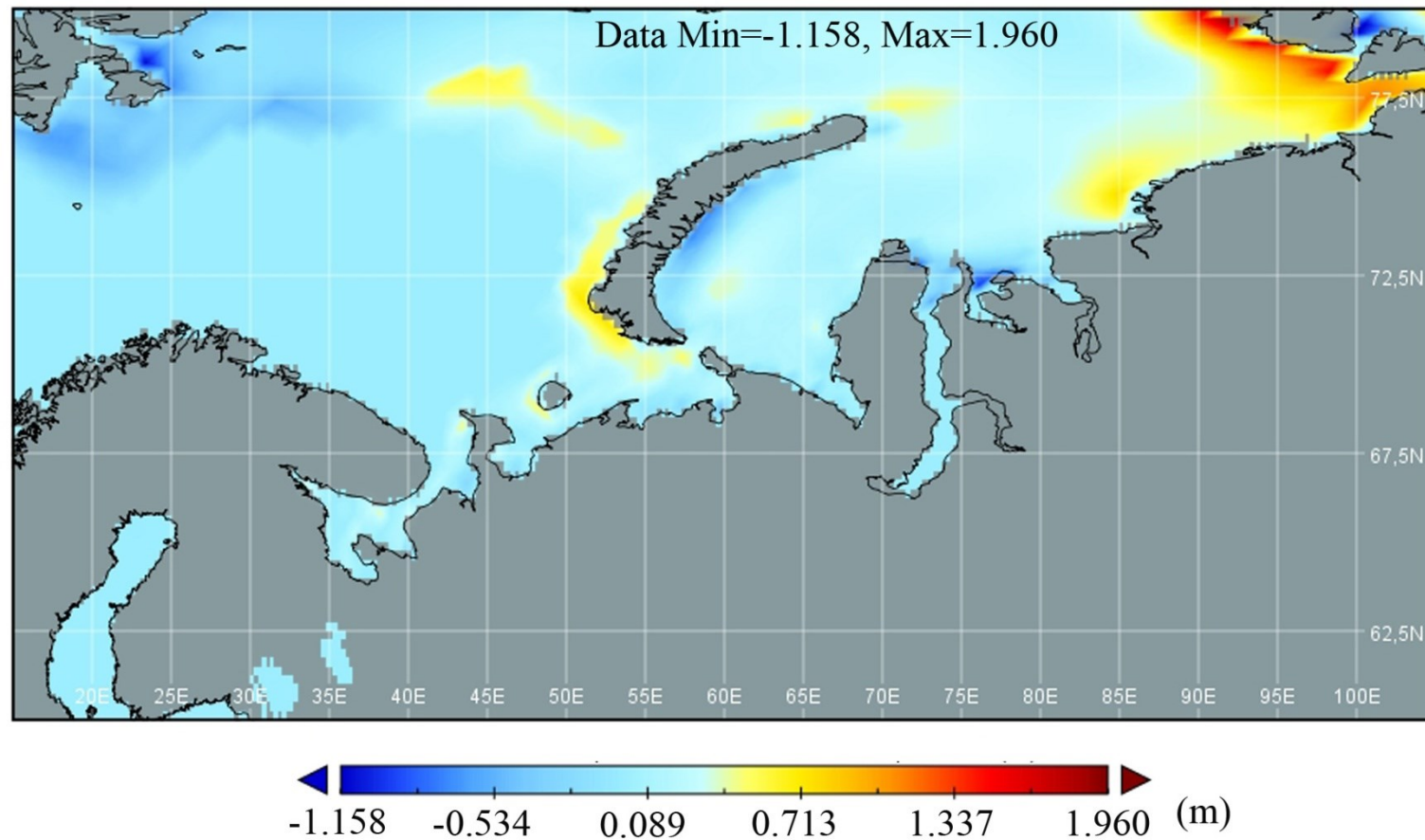
Annual Mean Temperature Change for Land and for Ocean NASA GISTEMP 2017 October

Annual Mean Temperature Change for Land and for Ocean

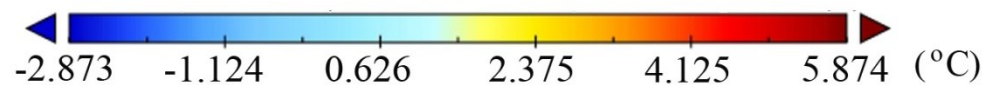
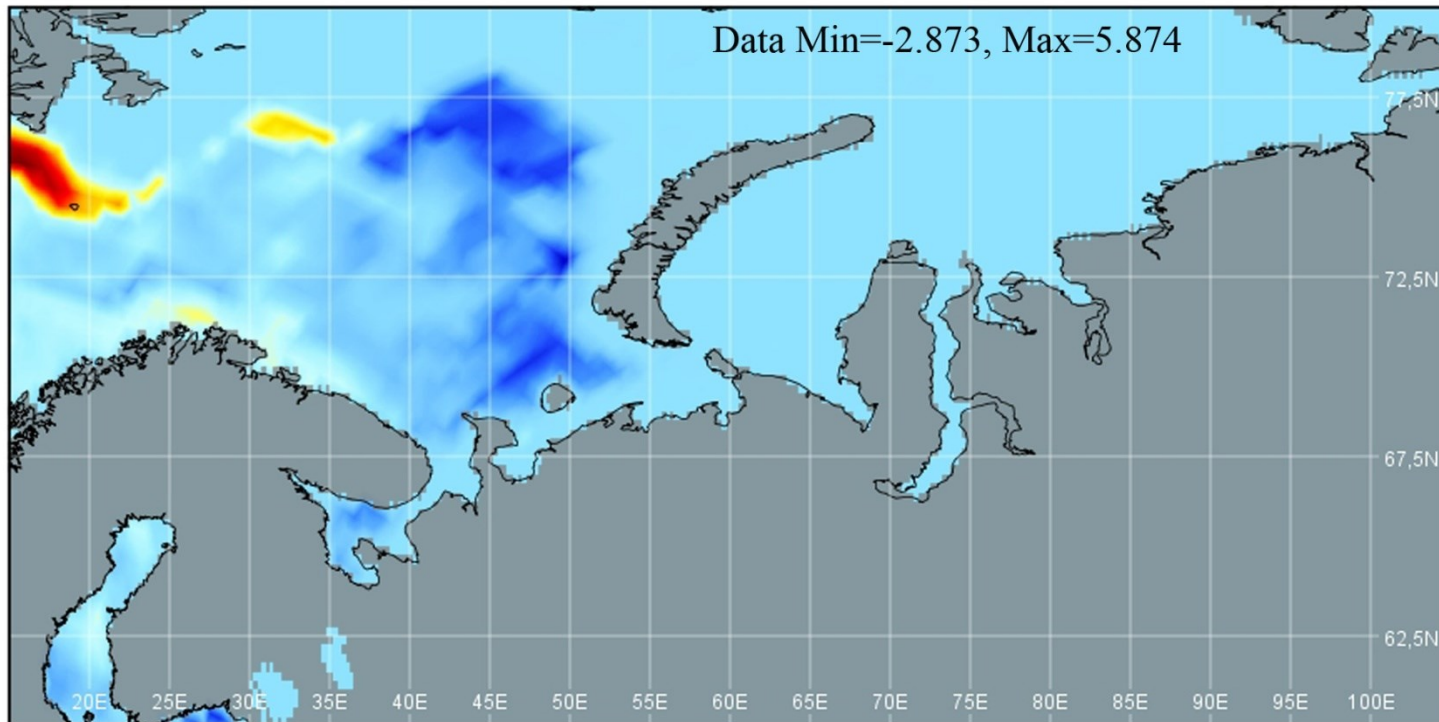


Annual (thin lines) and five-year lowess smooth (thick lines) for the temperature anomalies averaged over the Earth's land area and sea surface temperature anomalies averaged over the part of the ocean that is free of ice at all times (open ocean) <https://data.giss.nasa.gov/gistemp/graphs/>

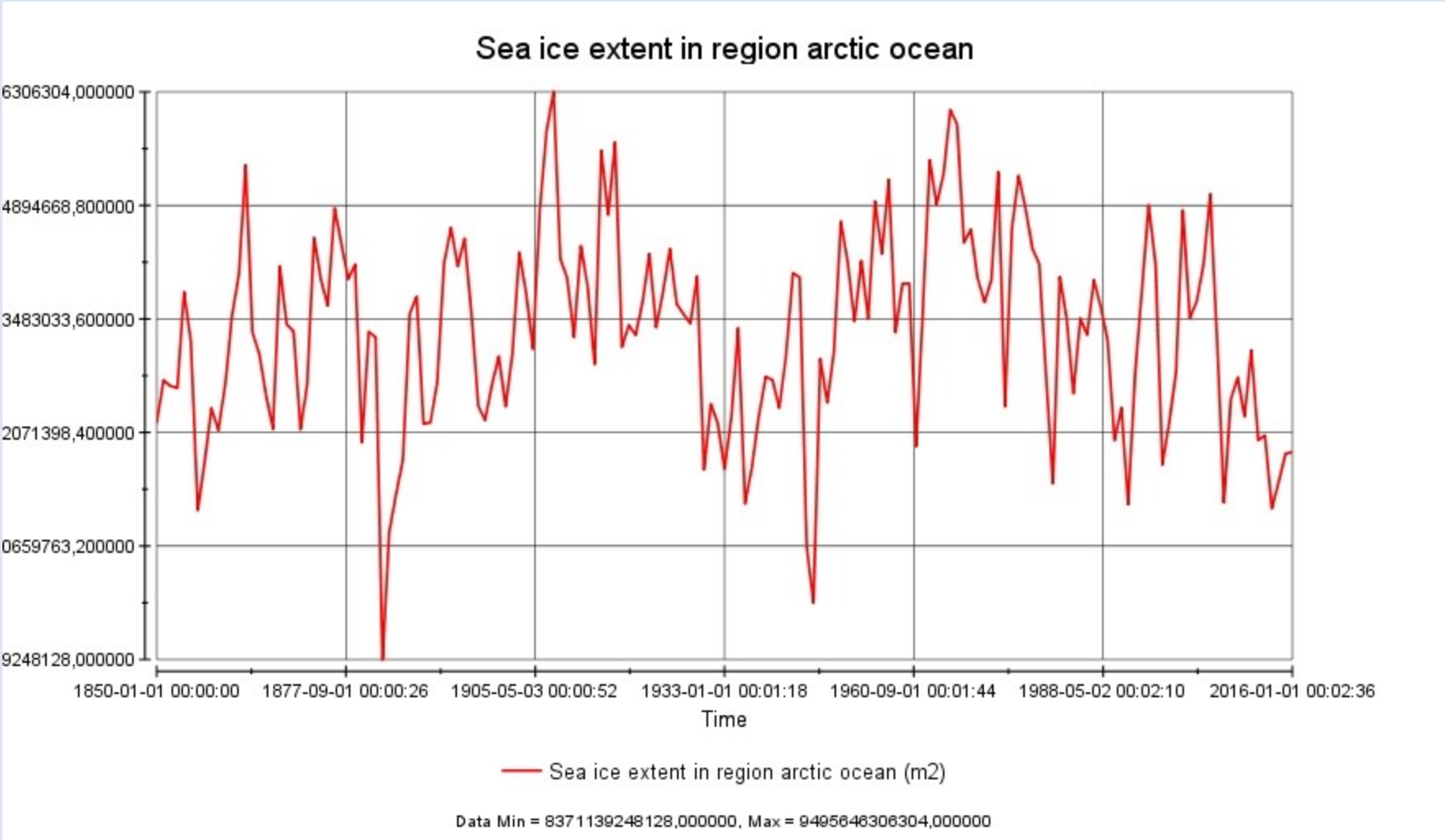
The difference of the ice fraction in the for Russian Arctic Zone 2000-2027 (model prediction) model MPI-ESM-HR in January



Potential temperature difference in Russian Arctic zone 2000-2027. Model MPI-ESM-HR in January



Change in the spread of ice cover in the Arctic zone 1850-2016 in January



Trends in numerical experiment in the coupled model

- As a result of this **temperature increase, ice melting** and other climatic processes occur, which are actively discussed in the scientific community and in the mass-media.
- We also note that the fact of an **increase in dispersion characterizes an increase in randomness in the behavior of natural processes**. In particular, this is seen in an increase in abnormally cold and abnormally hot seasonal temperatures in various parts of the planet.
- An increase in precipitation, the appearance of **abnormally strong winds, sand storms in uncharacteristic areas and in uncharacteristic seasons**.
- The reflection of the listed phenomena in the **results of numerical modeling is a consequence of the nonlinearity of the joint ocean-earth-atmosphere model under consideration**.
- From this nonlinearity, for example, it follows **that the average values of the characteristics during ensemble modeling do not coincide with the average values of the model itself**, which is a special object of research.
- Studies of this kind of nonlinear models are needed not only from the point of view of studying systems of nonlinear equations, but also for **understanding natural processes**.

Conclusion

- The carried out numerical experiments show that the computer modelling of the coupled ocean-atmosphere dynamics for a decadal period in generally coincides with the observed tendencies. Thus, the increase in temperature mostly pronounced in the high latitudes is simulated by the model but also is seen directly.
- The **decrease of ice coverage in Polar Zone** is shown both from the model and directly from satellite. However, details of these processes in not clear directly from observations but become more understandable from the model simulation. In particular, the non-uniform character of the temperature increase over the entire globe is produced by the model.
- The **misbalance between the sea level anomalies that leads to the additional global mass and heat transfer can also be calculated only indirectly, not from direct measurements.**
- All of those conclusions confirm that the model climate simulation is very important and should be continued with CMIP6 experiments

Thank you for the attention!